Applied Catalysis B: Environmental 188 (2016) 169–176

Contents lists available at ScienceDirect

Applied Catalysis B: Environmental

journal homepage: www.elsevier.com/locate/apcatb

Enhanced electrocatalytic hydrogen evolution reaction: Supramolecular assemblies of metalloporphyrins on glassy carbon electrodes

Camila Canales[a], Felipe Varas-Concha[b], Thomas E. Mallouk[c,*], Galo Ramírez[a,*]

[a] Facultad de Química, Departamento de Química Inorgánica, Pontificia Universidad Católica de Chile, Av. Vicuña Mackenna 4860, Casilla 306, Correo 22, Santiago, Chile
[b] Facultad de Ingeniería, Departamento de Ingeniería Química y Bioprocesos, Pontificia Universidad Católica de Chile, Chile
[c] Departments of Chemistry, Biochemistry and Molecular Biology, and Physics, The Pennsylvania State University, University Park, PA 16802, USA

ARTICLE INFO

Article history:
Received 12 November 2015
Received in revised form 20 January 2016
Accepted 26 January 2016
Available online 1 February 2016

Keywords:
Hydrogen evolution reaction
Metalloporphyrins
Glassy carbon electrodes
Supramolecular system
Graphene

ABSTRACT

Chemically modified electrodes formed by π-stacking of metalloporphyrins provide a stable and efficient electrocatalytic system for the hydrogen evolution reaction at pH 7.0. Metalloporphyrins M-OEP (M = Co(II), Cu(II), Zn(II), Ru(II), Fe(III) and Ni(II), OEP = 2,3,7,8,12,13,17,18-Octaethyl-21*H*,23*H*-porphine) were deposited on glassy carbon electrodes that had been previously modified by using NaOH and 4-aminopyridine, which served as a bridging molecule between the metalloporphyrins and the electrode surface. Different supramolecular architectures, as revealed by AFM and SEM, were obtained with bare and oxidized glassy carbon electrode surfaces. The most active systems were those obtained with Co(II) and Cu(II) porphyrins. Raman spectra showed the presence of the linking molecules and metalloporphyrins in the electrocatalytic metalloporphyrin films.

1. Introduction

A major issue in the development of renewable energy resources is the production of hydrogen (H_2) from sources other than fossil fuels. Currently, the most economical process for hydrogen production is steam reforming of natural gas, which entails the production of CO_2 as a byproduct [1,2]. Water electrolysis is recognized as an alternative, albeit expensive, method to obtain H_2, since it provides a link between electrical energy and hydrogen, a high-energy-density fuel and a versatile energy carrier [3–5]. The hydrogen evolution reaction (*her*) is the cathode reaction in water electrolysis and is one of the main determinants of cost and efficiency. Traditionally, the *her* has been catalyzed in membrane-based electrolyzers by precious metal catalysts, such as Pt, which are rare, expensive, and easily poisoned. More recently, electrocatalysts derived from earth-abundant transition metals such as Fe, Co and Ni have been investigated as promising alternatives in both acidic and alkaline electrolytes [6–11]. It is well documented that aza-macrocyclic compounds, such as metalloporhyrins, can catalyze many reactions due to their *redox* activity, chemical stability, and planar structure, among other characteristics [12]. A number of discrete molecular cobalt and nickel complexes have been found to electrocatalytically reduce water to hydrogen with high Faradaic yields [13–16], but most of these electrocatalysts have been studied in non-aqueous solutions. We show here that some of these materials can be used to modify electrodes and produce cathodes with high catalytic activity for hydrogen evolution from water.

In this work we have modified glassy carbon electrodes with commercial octaethylporphyrins (M-OEP, M = Co(II), Cu(II), Zn(II), Ru(II), Fe(III) and Ni(II)) in order to study their electrocatalytic properties in the aqueous hydrogen evolution reaction. Glassy carbon electrodes were covalently modified by surface oxidation and by reaction with 4-aminopyridine (4AP) with the aim of anchoring the catalytic molecules by coordination to the metal center of the porphyrin. This modification enables the deposition of molecular assemblies that are formed by π-stacking. In this supramolecular architecture, a synergic effect is expected since π-stacking provides good electronic communication between the electrode and catalytic sites in the metalloporphyrins. The morphology of these electrode films was characterized by Atomic Force Microscopy (AFM) and Scanning Electron Microscopy (SEM), and the structure of the supramolecular aggregates was studied by Raman spectroscopy. The Raman spectra verify the existence of the covalent

* Corresponding authors.
E-mail addresses: tem5@psu.edu (T.E. Mallouk), gramirezj@uc.cl (G. Ramírez).

http://dx.doi.org/10.1016/j.apcatb.2016.01.066
0926-3373/

Table 1
Tafel slopes calculated for GC + 4AP + Co(II)OEP, GC ox + Cu(II)OEP and GC + Cu(II)OEP at buffer phosphate solution, pH 7.0 (scan rate = 5 mV s^{-1}). Amount of porphyrin deposited on each system.

System	Tafel slope value (mV per decade)	Amount of M-OEP deposited (mol)
GC + 4AP + Co(II)OEP	194	4.86×10^{-8}
GC ox + Cu(II)OEP	103	5.22×10^{-8}
GC + Cu(II)OEP	90	3.65×10^{-8}

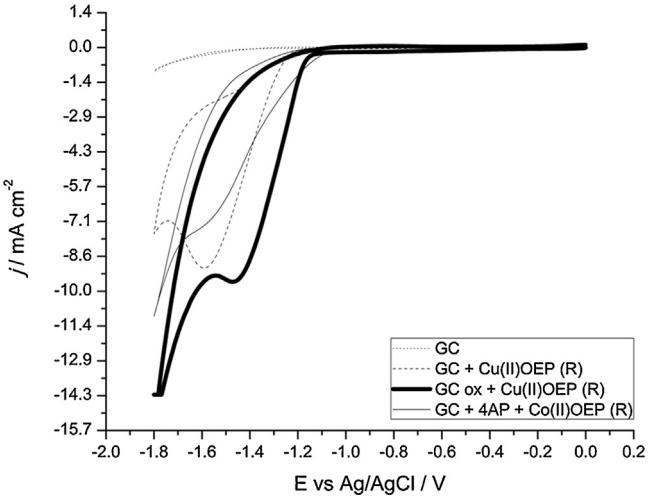

Fig. 1. Comparative CVs of bare and modified electrodes with the best electrocatalytical responses towards *her* at aqueous phosphate buffer solution, pH 7.0. Scan rate: 100 mV s^{-1}.

linkages between the electrode surface and metalloporphyrins through the 4AP molecule and oxidized groups.

2. Experimental

2.1. Chemicals and solutions

KCl, NaOH and Cl_2CH_2 were obtained from Merck as analytical grade reagents. Deionized water was obtained from a Millipore-Q system (18.2 MΩ cm). Argon (99.99% pure) and dioxygen gas were purchased from AGA, Chile. Metalloporphyrins (2,3,7,8,12,13,17,18-Octaethyl-21*H*,23*H*-porphine cobalt(II), 2,3,7,8,12,13,17,18-Octaethyl-21*H*,23*H*-porphine copper(II), 2,3,7,8,12,13,17,18-Octaethyl-21*H*,23*H*-porphine zinc(II), 2,3,7,8,12,13,17,18-Octaethyl-21*H*,23*H*-porphine ruthenium(II) carbonyl, 2,3,7,8,12,13,17,18-Octaethyl-21*H*,23*H*-porphine iron(III) chloride and 2,3,7,8,12,13,17,18-Octaethyl-21*H*,23*H*-porphine nickel(II)) and 4AP, were all purchased from Sigma-Aldrich Chile.

2.2. Instrumentation

Cyclic voltammetry studies were performed on a CH Instruments 750D potentiostat galvanostat. The conventional three-electrode system consisted of a glassy carbon (GC) working electrode (0.071 cm^2), Ag/AgCl (3 M KCl) reference electrode, and a platinum wire counter electrode. Gold electrodes were used in parallel experiments in order to obtain Raman spectra.

For electrolysis experiments, an electrolysis cell was used. A conventional three-electrode system was used, consisting of a glassy carbon (GC) working electrode (1.7 cm^2), Ag/AgCl (3 M KCl) reference electrode, and a platinum wire counter electrode. Gas chromatography experiments were carried out by using a DANI-Instruments® Gas Chromatograph.

Atomic Force Microscopy (AFM) studies were done by using an Innova® Atomic Force Microscope. Scanning Electron Microscopy (SEM) studies were performed in a Nova NanoSEM™ 630 and Raman spectra were obtained by using a Renishaw microRaman instrument.

2.3. Preparation of modified electrodes and analysis

The GC electrode was polished to a mirror finish on a felt pad using alumina slurries (3 μm). Then, it was cleaned by immersion in an ultrasonic bath for 60 s, and finally stabilized by cycling the potential between −0.7 V and 0.7 V in a solution of 0.1 M NaOH under Ar atmosphere.

Covalently modified electrodes were obtained as reported previously using NaOH and 4AP [10,17]. Then, they were submerged in a 0.2 mM solution of metalloporphyrin, M-OEP (M = Co(II), Cu(II), Zn(II), Ru(II), Fe(III) and Ni (II)) dissolved in CH_2Cl_2 for 20 min at room temperature (In) and for 60 min under reflux (R). The electrodes were then dried at room temperature for 1 min.

All the modified electrodes were analyzed in a phosphate buffer solution ($H_2PO_4^-/HPO_4^{2-}$ 0.066 mol L^{-1} saturated with Ar) by cycling the potential between 0.0 V and −1.8 V. Controlled-potential electrolyses at −1.1 V were conducted in stirred 0.066 mol L^{-1} phosphate buffer solutions, pH 7.0. The faradaic yield of H_2 was determined by sampling the headspace of the electrolysis cell after 4 h and analyzing the sample by gas chromatography.

Gold-coated glass slides (EMF Corp. CA134, 100 nm Au deposited onto a 5 nm Cr adhesion layer on float glass) were used as gold electrodes. These electrodes were cleaned with acetone in ultrasonic bath for 40 min before each modification, whereas graphene electrodes were used as received. Both substrates were stabilized on a 0.1 M NaOH solution by cycling the potential between −1.0 and 1.0 V, and −0.7 and 0.7 V, for gold and graphene electrodes respectively.

Raman spectra were obtained by modifying gold and graphene electrodes, following the same procedure used for glassy carbon electrodes. These substrates were used since GC is not appropriate for Raman studies. Laser excitation wavelengths of 786 nm (for studying bonding of 4AP to the electrode) and 532 nm (for supramolecular porphyrin complexes) were used.

Table 2
Quantification of total amount of H_2 produced by generated systems.

System	Peak area (mVs)	Total H_2 produced (μmol)	Total H_2 produced per time (μmol h^{-1})	Total H_2 produced per time and area (μmol h^{-1} cm^{-2})
GC	3.3	21.2	5.3	3.1
GC ox + Cu(II)OEP	616.0	169.8	42.5	25.0
GC + Cu(II)OEP	892.8	237.0	59.3	34.9
GC + 4AP + Co(II)OEP	1207.8	313.4	78.4	46.1

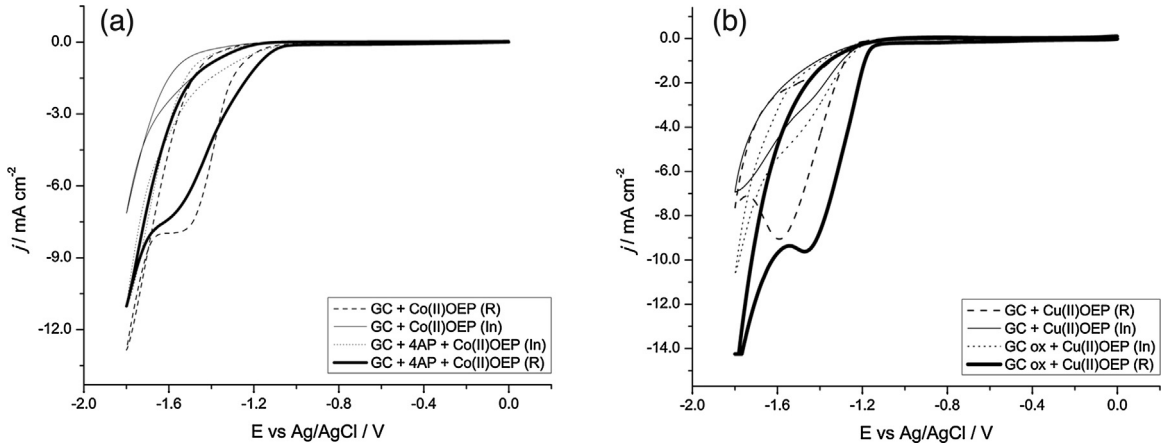

Fig. 2. CVs of modified electrodes with Co(II)OEP (a) and Cu(II)OEP (b) complexes at aqueous phosphate buffer solution, pH 7.0. Scan rate: 100 mV s^{-1}.

Morphological studies were done by using AFM and SEM. In these studies, all samples were analyzed on glassy carbon substrates. Tapping mode was used in all AFM experiments.

3. Results and discussion

3.1. Voltammetric measurements

In order to study the *her,* glassy carbon electrodes modified by 4AP were prepared in NaOH/4AP solutions as previously reported [17]. Then, two systems covalently modified are obtained: GC ox and GC + 4AP. In the first case, oxidized groups are formed on the GC surface [17,18] in order to serve as anchoring group between the electrode and the metalloporphyrin. Each metalloporhyrin studied was deposited via immersion (In) and reflux (R) (Figs. S1–S3, Supporting information), with the aim of comparing the effects of the bridging molecule, the catalytic metal center, and the method of electrode modification. The bridging molecule is covalently bonded to the carbon electrode surface and, at the same time, is coordinated to the metal center of the complex, which generates the first layer of complexes bonded to the electrode surface through the bridge molecule. On this first layer, more layers of complexes are stacked by π interactions that finally form a system with supramolecular characteristics [19]. Fig. 1 shows the voltammetric responses of the most active systems for the *her* after 10 cycles. The most active systems are those generated via reflux (R) with Co(II) and Cu(II) complexes (Fig. S4, Supporting information) over the ones generated by immersion and other metalloporphyrins. By comparing the (In) and (R) electrodes, it is evident that the method of modification strongly influences the electrocatalytic response towards the *her* (see Supporting information).

By using reflux as the method of modification, we expected to generate thicker assemblies or aggregates of complexes that are held together by π interactions. These architectures would promote electronic communication between the electrode and the catalytic metal centers in the metalloporphyrin complexes. The systems GC + 4AP + Co(II)OEP and GC ox + Cu(II)OEP have higher electroactivity than the other metalloporphyrins studied, providing evidence of the effect of the metal center. These metals are electron-rich atoms and their electronic configuration facilitates the charge transfer processes in order to reduce H^+ in aqueous media to produce H_2.

The obtained systems are as active as other 3d transition metal macrocyclic catalysts previously reported [15], and in comparison to earlier studies [16,20], the responses are better in terms of potential and current, considering the pH of the medium. These previous studies show that, as the pH is increased, the activity of the catalyst at constant overpotential decreases. Thus, a higher overpotential is required to reduce H^+ near neutral pH, and a more complex system is required to electrocatalyze the *her* because the reduction of the redox couple Co^{II}-Co^{I} occurs at higher overpotential. The metalloporphyrin films described here are simple to prepare, and are electroactive at pH 7.0.

As noted above, the refluxing method results in the formation of metalloporphyrin aggregates through π-stacking, and covalent anchoring to the electrode is expected to impart stability and directionality of electron flow in the system. In order to test this hypothesis, the voltammetric responses of the systems generated from Co(II) and Cu(II) complexes, in presence and absence of the 4AP anchoring molecule were studied, and the results are shown in Fig. 2. These comparisons confirm that substantial differences in electrocatalytic activity occur depending on the presence of the 4AP molecule and the method of electrode modification.

For both Co(II) and Cu(II) complexes, we observe an electroactivity enhancement when the electrode is modified with 4AP and when the film is deposited by the reflux method. These observations suggest that these new systems have a supramolecular character, due to the bridge molecule that orients the assemblies (by the coordination of the metal center which occupies an axial free position) and due to the reflux, which facilitates the aggregation of porphyrin films on the electrode surface [19,21,22].

A Tafel slope greater than 100 mV per decade was expected since a Tafel slope of about 160 mV per decade in aqueous electrolyte at neutral pH has been previously observed with related catalysts [23]. The Tafel slope at high negative overpotentials is consistent with *her* that proceeds via a Volmer-Heyrovsky mechanism [20,21,24], as follows:

$$M + H_3O^+ + e^- \rightarrow M - H_{ads} + H_2O \quad (1)$$

$$M - H_{ads} + H_3O^+ \rightarrow M + H_2 + H_2O \quad (2)$$

$$M - H_{ads} + M - H_{ads} \rightarrow H_2 + 2M \quad (3)$$

Table 1 shows the calculated values of Tafel slopes corresponding to each obtained system. In every case, the values are around 100 mV per decade, which is consistent of what is discussed before. The amount of metalloporphyrin deposited on the electrodes is also considered.

3.2. Efficiency studies

During steady-state electrolysis, the generation of bubbles on both sides of the cell was observed, which gives evidence of H_2 production on the GCE and O_2 production at the counter electrode. The results of this experiment are presented in Fig. 3. Over a 4 h

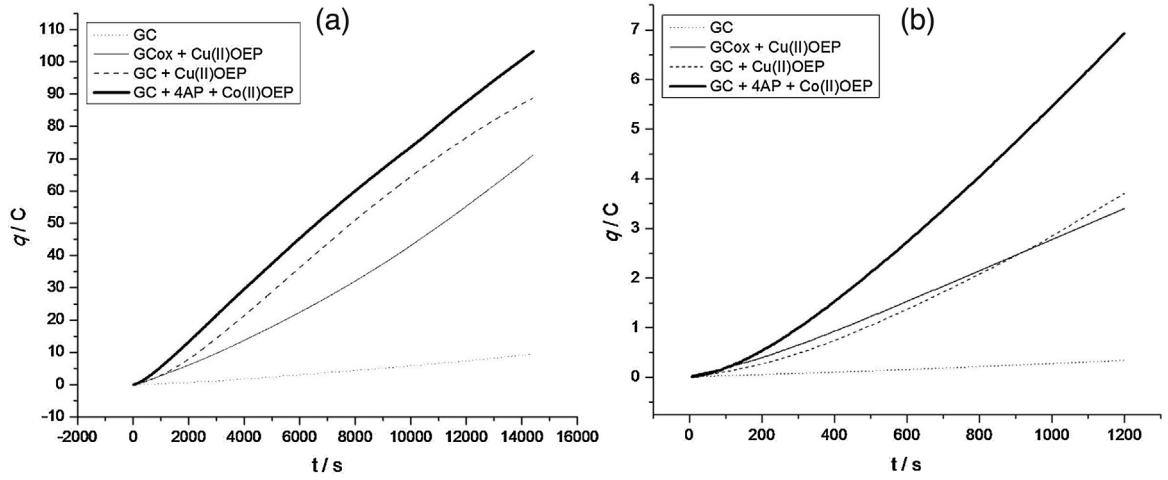

Fig. 3. Controlled potential electrolysis in aqueous solution at pH 7.0 of GC, GC ox + Cu(II)OEP, GC + Cu(II)OEP and GC + 4AP + Co(II)OEP showing accumulative charge over 4 h (a) and 20 min (b) with an applied potential of −1.1 V vs Ag/AgCl.

electrolysis period, we found that the GC + 4AP + Co(II)OEP system is the most active one with respect to H_2 production (Fig. 3). This result was not expected since cyclic voltammetry showed a better response with the GC ox + Cu(II)OEP system (Fig. 1). To explain this result, it is important to consider that voltammetry reports on the system behavior on short timescales and thus, electrolysis results should be compared at shorter periods of time. By considering this, we observed that the GC ox + Cu(II)OEP system is the most efficient only in the first 100 s (Fig. 3).

By integrating the charge passed in these systems, it is possible to determine the Faradaic efficiency, turnover number, and overpotentials, which compare favorably to systems previously reported [15,16,25,26]. In this sense, Hung and co-workers reported a system modified with a water-soluble anionic cobalt(II) tetrakis-(*p*-sulfonatophenyl) porphyrin (CoTPPS), previously synthesized [27]. Although this system has a high efficiency towards *her* at neutral pH, in this present work we have found that is possible to obtain as stable and efficient systems using commercial metalloporphyrins (M-OEP) adsorbed onto GC electrodes previously modified with anchoring groups. These novel systems are capable to reduce protons at low overpotentials at neutral pH, with comparable TONs. This result is due to the generation of a supramolecular system which possesses a synergic effect that means, they have a great electrocatalytic effect in comparison to the bare electrode and their monomers themselves. Then, if a monolayer is active, as the one demonstered by Hung et al. [27]. it would be posible to obtain a more active system.

Finally, in order to evaluate the efficiency of the catalytic systems. Tables 2 and 3 show the results obtained by gas chromatography.

Table 3
Obtained charge over 4-h electrolysis with generated systems and their corresponding faradaic efficiencies[a].

System	q^b/C	f^c/%	TON[d]
GC	7	58	–
GC ox + Cu(II)OEP	55	61	3.3×10^3
GC + Cu(II)OEP	80	58	6.5×10^3
GC + 4AP + Co(II)OEP	102	60	6.4×10^3

[a] All experiments were done twice at −1100 mV vs Ag/AgCl (average showed).
[b] Total amount of charge obtained.
[c] Faradaic efficiencies determined by gas chromatography.
[d] Turnover number calculated with total amount of hydrogen produced by moles of electrocatalyst.

The GC + 4AP + Co(II)OEP modified system is the one that generates more charge over 4 h electrolysis, with a faradaic efficiency of 60%, which corresponds to 6400 turnovers of the catalyst. The other systems have a similar efficiency, and their TONs are similar or lower (GC ox + Cu(II)OEP). These results give evidence of the electroreduction of water to hydrogen, but at lower rates. Additionally, in all electrolysis experiments, the current was constant, which indicates that the electrocatalyst is stable under these conditions. An example of this behavior is shown in Fig. 4, where the system is shown to be stable by applying a negative fixed potential for several minutes.

This last result is consistent with voltammetric profiles obtained after 10 cycles (Fig. 1).

3.3. Morphological studies

AFM studies were performed in order to analyze morphological changes on carbon surfaces. Fig. 5 illustrates the images obtained. The AFM images support the idea that the covalent bond is important for generating molecular stacks on the carbon surface, since the direct deposition of the metalloporphyrin shows a different

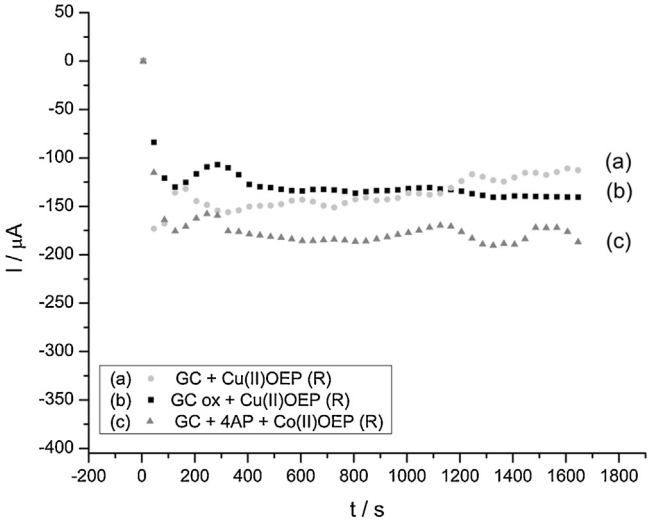

Fig. 4. Superposition of the chronoamperometric curves for GC modified electrodes at −1.7 V in a 0.066 M phosphate buffer solution, pH 7.0, purged in Ar. Total time of experiment: 1700 s.

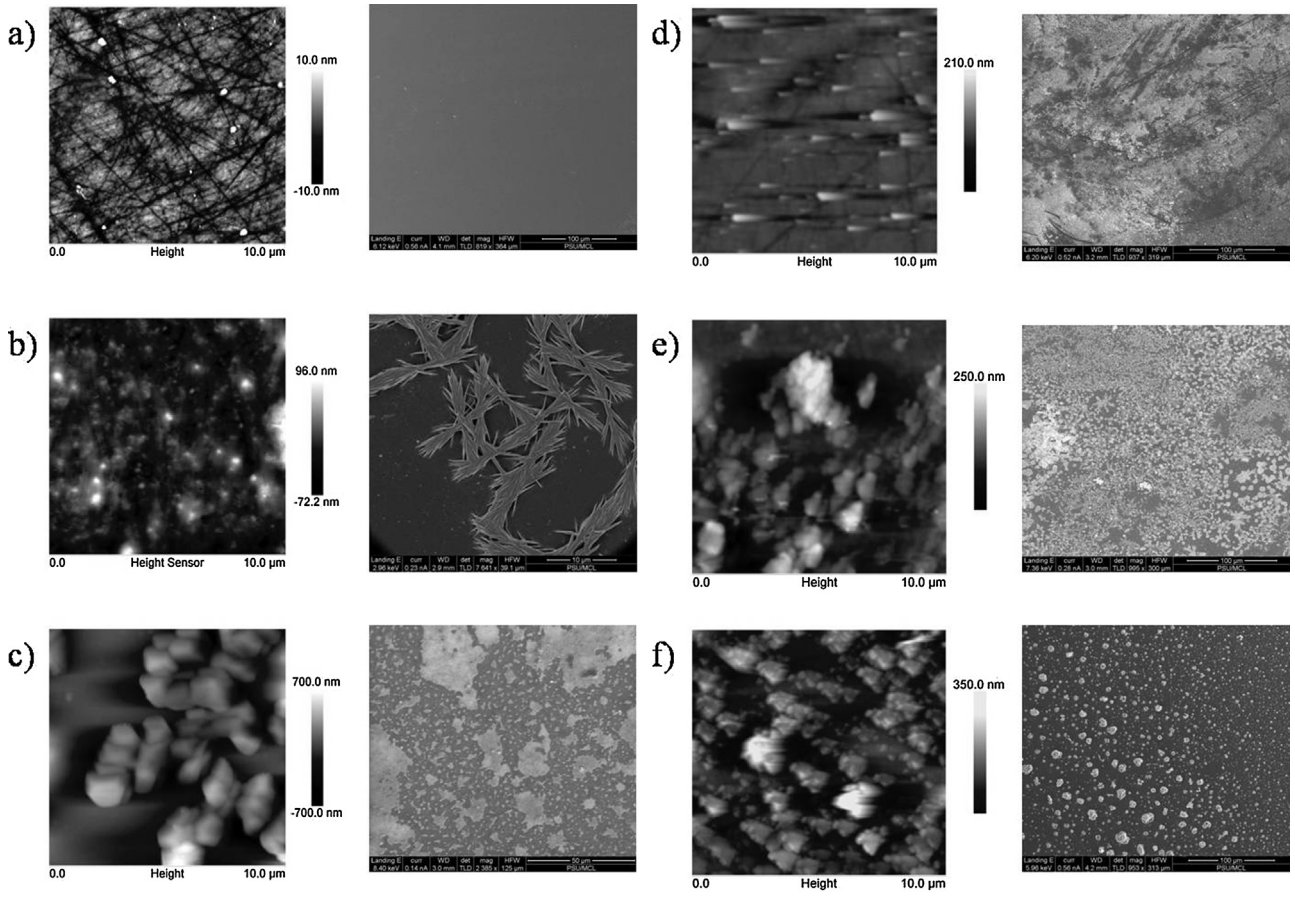

Fig. 5. AFM and SEM images of (a) bare GCE and modified GCEs: (b) oxidized GC (GC ox), (c) GC + 4aminopyridine (GC + 4AP), (d) GC + Cu(II)OEP, (e) GC ox + Cu(II)OEP, (f) GC + 4AP + Co(II)OEP.

Table 4
Rq values corresponding to the bare GC and modified GC electrodes.

System	Rq value (nm)
GC	2.54
GC ox	19.6
GC + 4AP	177
GC + AP + Co(II)OEP	55
GC ox + Cu(II)OEP	38.3
GC + Cu(II)OEP	16.8

morphology that keeps the surface relatively flat. This effect can be corroborated by comparing the *Rq* values obtained in this study, which are showed in Table 4 and which stand for root-mean-square roughness (RMS).

Since *Rq* is the standard deviation of the height, it describes the spread of the height distribution about the mean value [28,29]. SEM studies were performed as well, with the aim of corroborate the morphological behavior of the samples. For each modified electrode, Fig. 5 shows its corresponding SEM image.

it is known, the surface chemistry of sp^2 carbon materials is governed by basal and edge carbon atoms [30,31], as well as by the presence of defects (i.e., structural carbon vacancies, non-aromatic rings) [32], then, heteroatoms, such as oxygen and nitrogen, can be chemisorbed, leading to stable surface compounds, and resulting in a complex surface chemistry. This last effect is obtained once the carbon electrode is modified with covalent bonds, and so they can act as new active sites for porphyrin deposition (Fig. 5b and c).

However, it can be seen that still the chemiadsorption of Cu(II)OEP is achieved without using a covalent bond (Fig. 5d). This is a result of the nature of porphyrins (and other macrocycles), which are capable of forming π interactions with carbon by their own. Though this direct deposition might affect the electronic properties of the Cu(II) porphyrin, the advantage is that this synthetic strategy does not require any prior chemical modification [33].

Fig. 6 shows images corresponding to the modified electrodes and the comparison between methods of modification. There are obvious differences between the samples modified by immersion and those modified by reflux, which are the responsible of the electrocatalitic response towards *her*. In this sense, the refluxed systems can give a different morphology of the entire system that helps to carry the electron transfer out.

3.4. Structural studies: Raman spectroscopy

Raman spectra were obtained to study the linkage between the electrode, oxidized groups, the 4AP molecule, and metalloporhyrins. In this study, gold and graphene electrodes were used with the aim of obtaining better responses by using the Raman technique. The electrodes were modified as was done for glassy carbon electrodes, and the modifications were corroborated by electrochemical responses.

Molecular vibrations of the four-coordinate planar metalloporphyrins are classified into the in-plane and out-plane modes, in which A_{1g}, B_{1g}, B_{2g} and E_g modes are Raman active. However, in resonance with B_0 and Q_0 bands, these modes are expected to gain Raman intensity [34].

Also, it is possible to consider the Raman spectra for modified electrodes with covalent bonds. At this point, oxidized groups can be recognized at 1034 and 576 cm^{-1} [35] and chemisorbed pyridine [36] gives their corresponding frequencies as shown in Table 5.

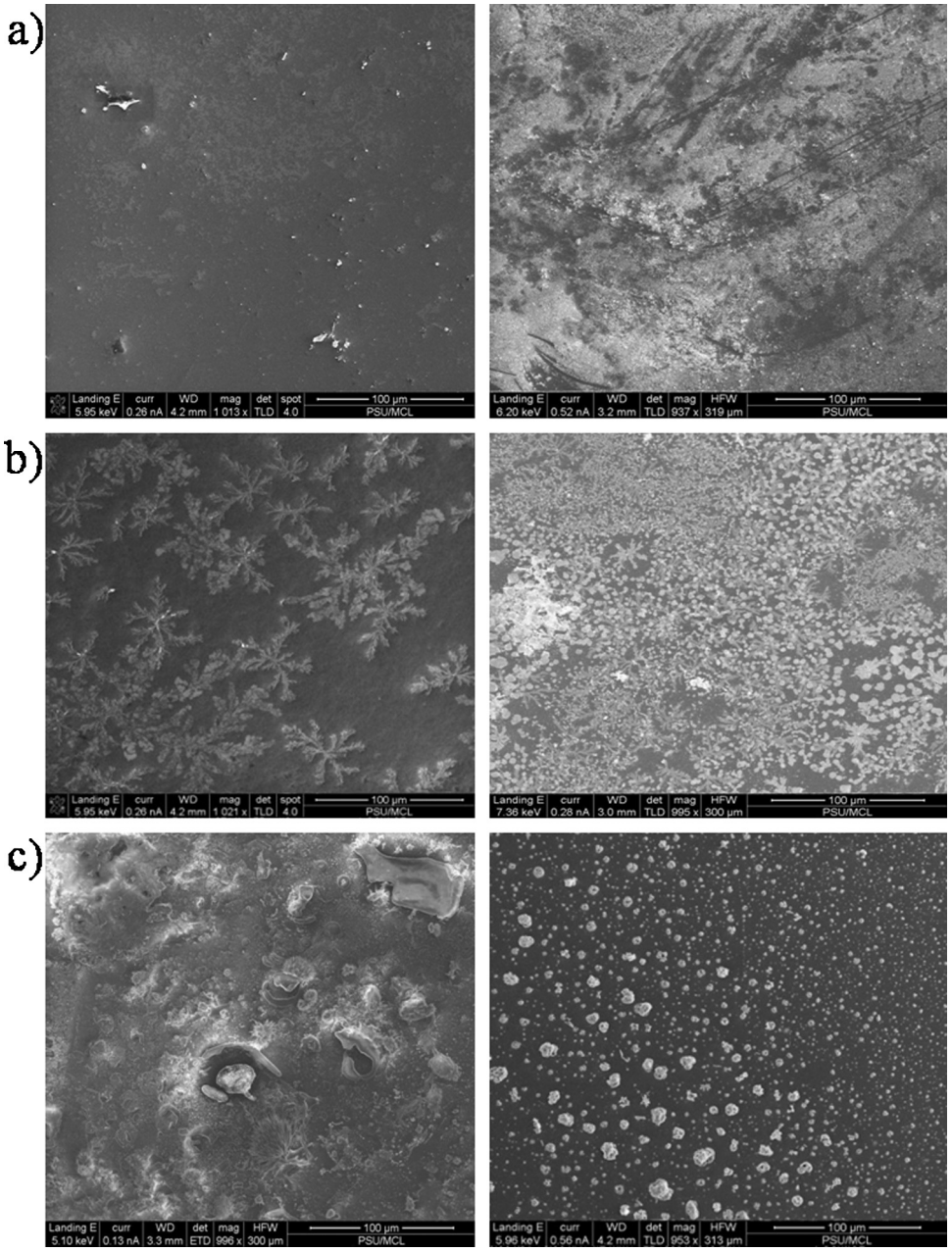

Fig. 6. SEM images of (a) GC + Cu(II)OEP (In) and GC + Cu(II)OEP (R), (b) GC ox + Cu(II)OEP (In) and GC ox + Cu(II)OEP (R), (c) GC + 4AP + Co(II)OEP (In) and GC + 4AP + Co(II)OEP (R).

These modifications enable the linkage to the gold electrodes, by acting as new active sites. It is possible to observe the differences between spectra obtained with the anchoring molecule only and spectra obtained after the metalloporhyrin deposition. These latter spectra show characteristic frequencies for metalloporphyrins (Table 5), but also, it is possible to recognize that there are shifts occurring at Raman frequencies by comparing the systems obtained by immersion and reflux. This provides additional evidence that there are structural differences between films prepared by the two methods.

For supramolecular systems obtained in this study (and the pure reagents as well), the totally symmetric C—C stretching mode appears around 1475–1510 cm^{-1}. The peak around 1360–1375 cm^{-1} is attributed to the totally symmetric C—N stretching mode and this band may be referred to reflect π delocalization; as the extent of the d_π electrons to the LUMO of the porphyrin increases, its frequency decreases [37,38]. Due to the metal-axial ligand interactions, some Raman bands are affected. In this sense, C—N interactions are important in order to recognize the metal-axial ligand coordination. The stronger the Metal-*N*(pyrrole) bond, the shorter distance between the center of the porphyrin and the *N*(pyrrole) and the higher the ring stretching frequencies. When an axial ligand of the metalloporphyrin is occupied, a repulsive interaction between the ligand and pyrrole nitrogens occur which correspond to the repulsive interaction between the $d_x{}^2$-$d_y{}^2$ (metal) and $2p_{x,y}$ (N) orbitals [39]. Finally, it is possible to compare the pure reagent spectra with the results obtained in Fig. 7. C—N interactions appear around 1390 cm^{-1} and 1406 cm^{-1} (non-shown) for Cu(II)OEP and Co(II)OEP pure reagents, respectively. These latter results give evidence that the change of the C—N frequency in supramolecular systems is a result of coordination between the porphyrin and the covalently bound molecule

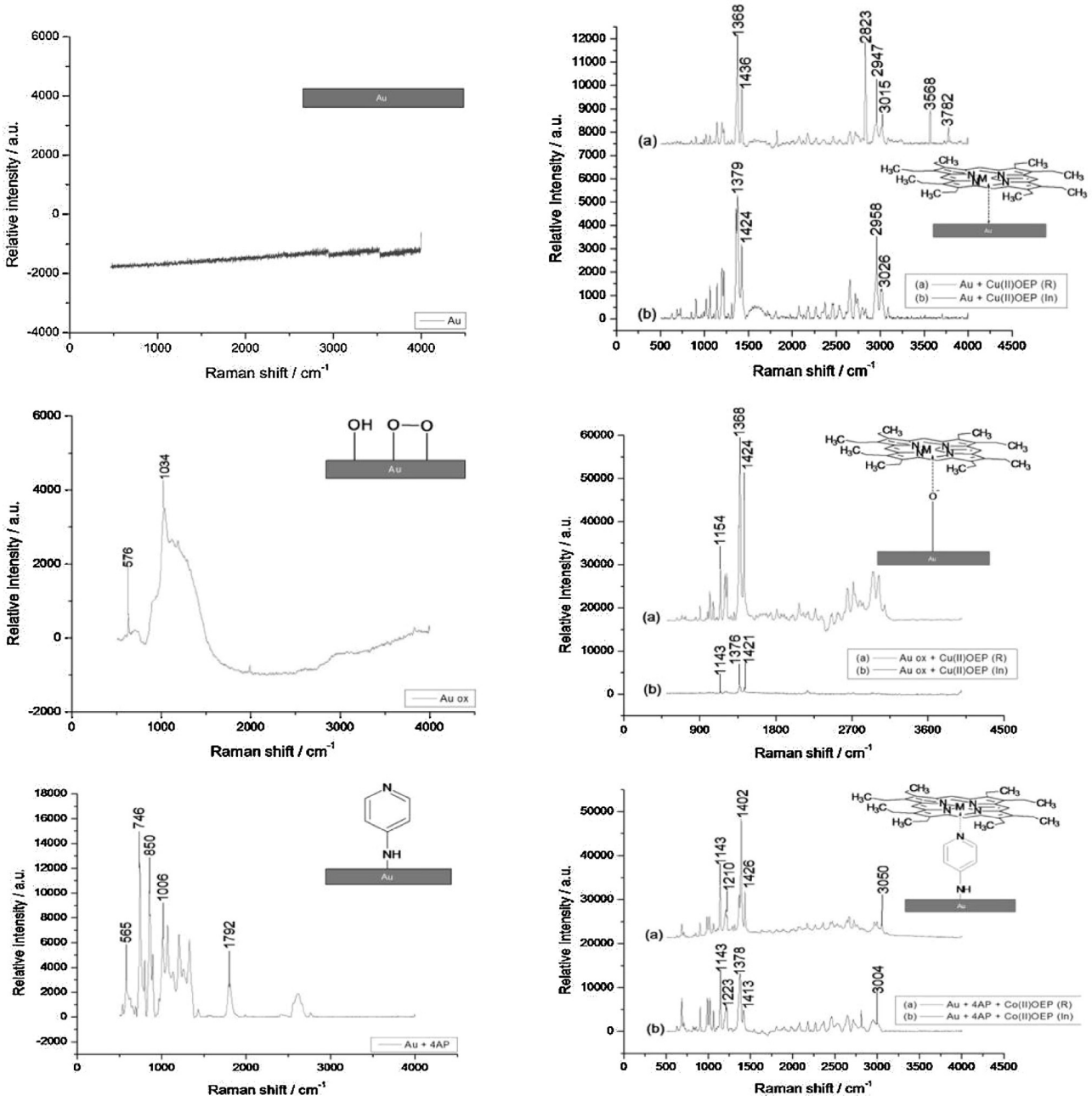

Fig. 7. Raman spectras of bare electrode (Au) and different modified electrodes. λ_{exc} = 786 nm (in absence of porphyrins), 532 nm (in presence of porphyrins).

on the electrode surface. Finally, Fig. 8 shows results obtained for graphene electrodes, which also present a good electroactivity and stability towards *her* when these substrates are modified to generate supramolecular systems as the ones presented here (Fig. S5, Supporting information).

With these results, it is possible to corroborate the generation of supramolecular systems, which imply an electrodic substrate (GC), the existence of an anchoring group and the coordination of metalloporphyrins through the metallic center. This system finally possesses a high stability due to the generation of a covalent bond previous to the porphyrin deposition, and with high efficiency towards hydrogen production.

Here, there is evidence of the modification of the graphene monolayers with the supramolecular catalysts.

4. Conclusions

The generated systems with covalent bonds and direct deposition via reflux behave as good electrocatalysts towards *her* and are highly efficient in comparison to other reported systems with similar molecular structures. This effect is attributed to the supramolecular structure of the electrode films, which facilitates the diffusion of reactants and products and the charge transfer processes. AFM and SEM studies show how the morphological behavior changes when different methods of modification are applied (immersion and reflux) and also, when covalent bonds are formed at the electrode surface prior to porphyrin deposition. Finally, Raman studies prove the existence of covalent bonds and the formation of supramolecular complexes on gold and graphene electrode surfaces, which are consistent with the electrocatalytic activity of the films towards *her*.

Table 5
Raman assignments for different systems (α = in plane bends, γ = out of plane bend, ν = stretch, δ = deformation vibration about the C_2 axis of pyrrole ring).

System	Raman shift/cm^{-1}	Assignment
Au-ox	1034	ν (OO)
	576	ν (OH)
Au + 4AP	1792	ν (CC)
	1006	α (CCC), ν (CC)
	850	γ (CH)
	746	Ring bend
	565	α (CCC)
Au + Cu(II)OEP (In)	3026	ν(CH)
	2958	ν (CH)
	1424	ν (CC), ν (C-Et)
	1223	δ (CH), ν (C-Et)
	1379	ν (CN), δ (C-C)
Au + Cu(II)OEP (R)	3782	ν (CH)
	3568	ν (CH)
	3015	ν (CH)
	2947, 2823	ν (CH)
	1436	ν (CC), ν (C-Et)
	1210	δ (CH), ν (C-Et)
	1368	ν (CN), δ (CC)
Au ox + Cu(II)OEP (In)	1421	ν(CC), ν (C-Et)
	1376	ν (C—N), δ (C—C)
	1143	ν (CN), δ (C-Et)
Au ox + Cu(II)OEP (R)	1424	ν (CC), ν (C-Et)
	1368	ν (CN), δ (CC)
	1154	ν (CN), δ (C-Et)
Au + 4AP + Co(II)OEP (In)	3004	ν(CH)
	1413	ν (CC), ν (C-Et)
	1378	ν (CN), δ (CC),
	1223	δ (CH), ν (C-Et)
	1143	ν(CN), δ (C-Et)
Au + 4AP + Co(II)OEP (R)	3050	ν (CH)
	1426	ν (CC), ν (C-Et)
	1402	ν(CN), δ (CC),
	1210	δ (CH), ν (C-Et)
	1143	ν (CN), δ (C-Et)

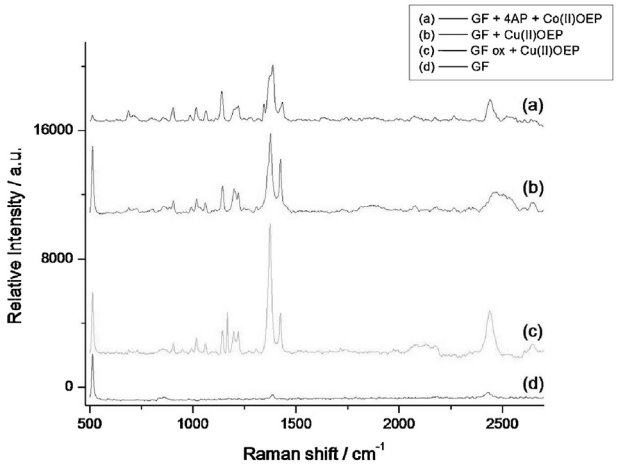

Fig. 8. Raman spectras of bare graphene (GF) and different modified electrodes. λ_{exc} = 532 nm.

Acknowledgements

The authors would like to acknowledge the financial support provided by FONDECYT Project No.: 1120049 and No.: 1141199, Doctoral Scholarship CONICYT Project No.: 21140095 and Project RC 130006, CILIS.

TEM acknowledges support from the Office of Basic Energy Sciences, Division of Chemical Sciences, Geosciences, and Energy Biosciences, Department of Energy under contract DE-FG02-07ER15911

Appendix A. Supplementary data

Supplementary data associated with this article can be found, in the online version, at http://dx.doi.org/10.1016/j.apcatb.2016.01.066.

References

[1] D.A.J. Rand, J. Solid State Electrochem. 15 (2011) 1579–1622.
[2] G. Everett, S. Boyle, Energy Systems and Sustainability: Power for a Sustainable Future, Oxford Univerity Press, 2012.
[3] S.P.S. Badwal, S.S. Giddey, C. Munnings, A.I. Bhatt, A.F. Hollenkamp, Front. Chem. 2 (2014) 79.
[4] C.G. Morales-Guio, L.-A. Stern, X. Hu, Chem. Soc. Rev. 43 (2014) 6555–6569.
[5] X. Chen, D. Wang, Z. Wang, P. Zhou, Z. Wu, F. Jiang, Chem. Commun. 50 (2014) 11683–11685.
[6] J. Deng, P. Ren, D. Deng, L. Yu, F. Yang, X. Bao, Energy Environ. Sci. 7 (2014) 1919–1923.
[7] D. Wang, J.T. Groves, PNAS 110 (2013) 15579–15584.
[8] F.J. Callejas, J.M. McEnaney, C.G. Read, J.C. Crompton, A.J. Biacchi, E.J. Popczun, T.R. Gordon, N.S. Lewis, R.E. Schaak, ACS Nano 8 (2014) 11101–11107.
[9] P. Jiang, Q. Liu, Y. Liang, J. Tian, A.M. Asiri, X. Sun, Angew. Chem. Int. Ed. 53 (2014) 1–6.
[10] A. Krawicz, J. Yang, E. Anzenberg, J. Yano, I.D. Sharp, G.F. Moore, J. Am. Chem. Soc. 135 (2013) 11861–11868.
[11] X. Wang, Y.V. Kolenko, L. Liu, Chem. Commun. 51 (2015) 6738–6741.
[12] J.H. Zagal, F. Bedioui, J.-P. Dodelet, N_4—Macrocyclic Metal Complexes, Springer Science—Business Media LLC, New York, 2006.
[13] X. Hu, B.S. Brunschwig, J.C. Peters, J. Am. Chem. Soc. 129 (2007) 8988–8998.
[14] X. Hu, B.M. Crossairt, B.S. Brunschwig, N.S. Lewis, J.C. Peters, Chem. Commun. 37 (2005) 4723–4725.
[15] C.C.L. McCrory, C. Uyeda, J.C. Peters, J. Am. Chem. Soc. 134 (2012) 3164–3170.
[16] A. Koca, Electrochem. Commun. 11 (2009) 838–841.
[17] C. Canales, L. Gidi, G. Ramírez, Int. J. Electrochem. Sci. 10 (2015) 1684–1695.
[18] T. Atogushi, A. Aramata, A. Kazusaka, M. Enyo, J. Electroanal. Chem. 318 (1991) 309–320.
[19] G. Ramírez, G. Ferraudi, Y.-Y. Chen, E. Trollund, D. Villagra, Inorg. Chim. Acta 362 (2009) 5–10.
[20] C.C. Vaduva, N. Vaszilcsin, A. Kellenberger, M. Medeleanu, Int. J. Hydrogen Energ. 36 (2011) 6994–7001.
[21] G. Ramírez, M. Lucero, A. Riquelme, M. Villagrán, J. Costamagna, E. Trollund, M.J. Aguirre, J. Coord. Chem. 57 (2004) 249–255.
[22] N. Navarrete, C. Canales, R. Del Rio, G. Ramírez, J. Chil. Chem. Soc. 58 (2013) 1971–1975.
[23] D. Voiry, H. Yamaguchi, J. Li, R. Silva, D.C.B. Alves, T. Fujita, M. Chen, T. Asefa, V.B. Shenoy, G. Eda, M. Chhowalla, Nat. Mater. 12 (2012) 850–855.
[24] A. Lasia, A. Rami, J. Electroanal. Chem. 294 (1990) 123–141.
[25] A.N. Frumkin, Hydrogen overvoltage and adsorption phenomena, in: P, Delahay, C.W. Tobias (Eds.), Advances in Electrochemistry and Electrochemical Engineering, vol. 3, Interscience Publishers Inc, New York, 1963, pp. 65–122.
[26] P.V. Bernhardt, L.A. Jones, Inorg. Chem. 38 (1999) 5086–5090.
[27] B.B. Beyene, S.B. Manea, C.-H. Hung, Chem. Commun. 51 (2015) 15067–15070.
[28] H. Wenhao, C. Yuhang, J. Phys. Conf. Ser. 13 (2005) 44–50.
[29] C. Canales, G. Ramírez, Electrochim. Acta 173 (2015) 636–641.
[30] L.R. Radovic, B. Bockrath, J. Am. Chem. Soc. 127 (2015) 5917–5927.
[31] M. Acik, Y.J. Chabal, Jpn. J. Appl. Phys. 50 (2011) 070101.
[32] F. Banhart, J. Kotakoski, A.V. Krasheninnikov, ACS Nano 5 (2010) 26–41.
[33] M.R. Axet, O. Dechy-Cabaret, J. Durand, M. Gouygou, P. Serp, Coord. Chem. Rev. (2015), http://dx.doi.org/10.1016/j.ccr.2015.06.005.
[34] J.W. Buchler, Metal complexes with tetrapyrrole ligands I, structure and bonding, in: T. Kitagawa, Y. Ozaki (Eds.), Infrared and Raman Spectra of Metalloporphyrins, vol. 64, Springer, Berlin, Heidelberg, 1987, pp. 71–114.
[35] P.J. Murphy, G. Stevens, M.S. Lagrange, Geochim. Cosmochim. Acta 64 (2000) 479–494.
[36] M. Fleischmann, I.R. Hill, J. Electroanal. Chem. 146 (1983) 353–365.
[37] T.G. Spiro, T.C. Strekas, J. Am. Chem. Soc. 96 (1974) 338–345.
[38] T. Kitagawa, T. Iizuka, M. Saito, Y. Kyogoku, Chem. Lett. 4 (1975) 849–852.
[39] J. Kincaid, K.J. Nakamoto, Inorg. Nucl. Chem. 37 (1975) 85–89.